JACS Au
AN OPEN ACCESS JOURNAL OF THE AMERICAN CHEMICAL SOCIETY

pubs.acs.org/jacsau
Article

Long-Range Interaction between Molecules with Electronic Degeneracy: Beyond the Born−Oppenheimer Approximation

Yipeng Yu, Xixi Hu,* Hua Guo,* and Daiqian Xie*

Cite This: *JACS Au* 2025, 5, 5079−5088
Read Online

ACCESS | Metrics & More | Article Recommendations | Supporting Information

ABSTRACT: Long-range intermolecular interaction plays an essential role in (ultra)cold collisions. For monomers with degenerate electronic states, an accurate description of the long-range interaction can be challenging due to the potential breakdown of the Born−Oppenheimer approximation. In this work, we developed a general method to construct long-range interaction potential energy surfaces (IPESs) between arbitrary molecules using the degenerate perturbation theory of Schrödinger. To further simplify the application of this method, a group-theoretical method is introduced to identify nonzero components of electrostatic properties of monomers, especially for the nonlinear molecules. To demonstrate this approach, we report the long-range IPESs of the O(^{3}P)−OH($^2\Pi$) and OH($^2\Pi$)−OH($^2\Pi$) systems. The excellent agreement with *ab initio* calculations in large separations, even near electronic degeneracies, confirms the accuracy of our approach. The method is expected to lay the groundwork for the accurate investigation of (ultra)cold collisional dynamics involving open-shell species.

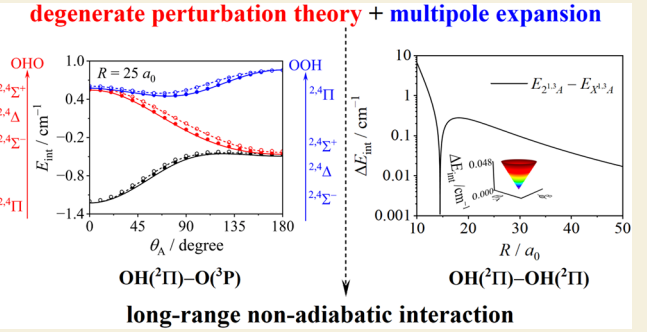

KEYWORDS: *intermolecular interaction, cold and ultracold collisions, potential energy surface, long-range interaction, molecular dynamics*

1. INTRODUCTION

Cold and ultracold collisions between molecules (or atoms) serve as a unique platform for investigating the quantum nature of molecular dynamics and for achieving accurate control of molecular scattering at the quantum state level.[1−7] At low temperatures, the long translational de Broglie wave probes the interaction potential energy surface (IPES) in the long-range.[5,6,8−11] In recent studies of the ultracold KRb + KRb → K_2 + Rb_2 reaction, for example, both reactivity and product state distributions are shown to be exquisitely controlled by long-range interactions.[12,13] Thus, a highly accurate IPES is vital for theoretical understanding of cold and ultracold collisions.[14]

When two molecules are sufficiently apart, the exchange interaction between the monomers can be neglected because it vanishes faster than any power of $1/R$, where R is the distance between them.[15] Thus, their interaction is dominated by electrostatic and dispersion forces. When two molecules are in nondegenerate states, in particular, the long-range interaction can be expressed in a multipole expansion as a sum of R^{-n} terms.[16,17] This analytical approach avoids direct *ab initio* calculations of the IPES in the long range, which can be quite challenging, guaranteeing physically correct behavior in the long range. Recently, we developed a general approach for constructing the long-range IPES between monomers in their nondegenerate electronic states.[18] (A similar approach has been established by Dawes and co-worker (R. Dawes, private communication)). This method, which is implemented in the program ABLRI, is based on Schrödinger's nondegenerate perturbation theory. Hence, it is not amenable to systems containing monomers with electronic degeneracy, which often lead to the violation of the Born−Oppenheimer approximation (BOA).[19]

Molecules involved in low-temperature reactions typically contain unpaired electrons, which often lead to barrierless reaction paths. For example, a much-studied case is the interaction between O(^{3}P) and OH($^2\Pi$),[20−22] which have spatial degeneracies of 3 and 2, respectively. As shown below, the multiple degenerate electronic states in the O + OH asymptote lead to the breakdown of the BOA, which destroys the simple analytical properties of the IPES. The proper treatment of these complications is thus of great importance for and challenge to understanding collisional dynamics in cold and ultracold conditions.

Over the past few decades, there have been several studies of the long-range interaction involving monomers in degenerate states by using degenerate perturbation theory.[19,21−37] However, most are system specific, aiming at atom−atom,[26−28]

Received: July 31, 2025
Revised: September 5, 2025
Accepted: September 8, 2025
Published: September 25, 2025

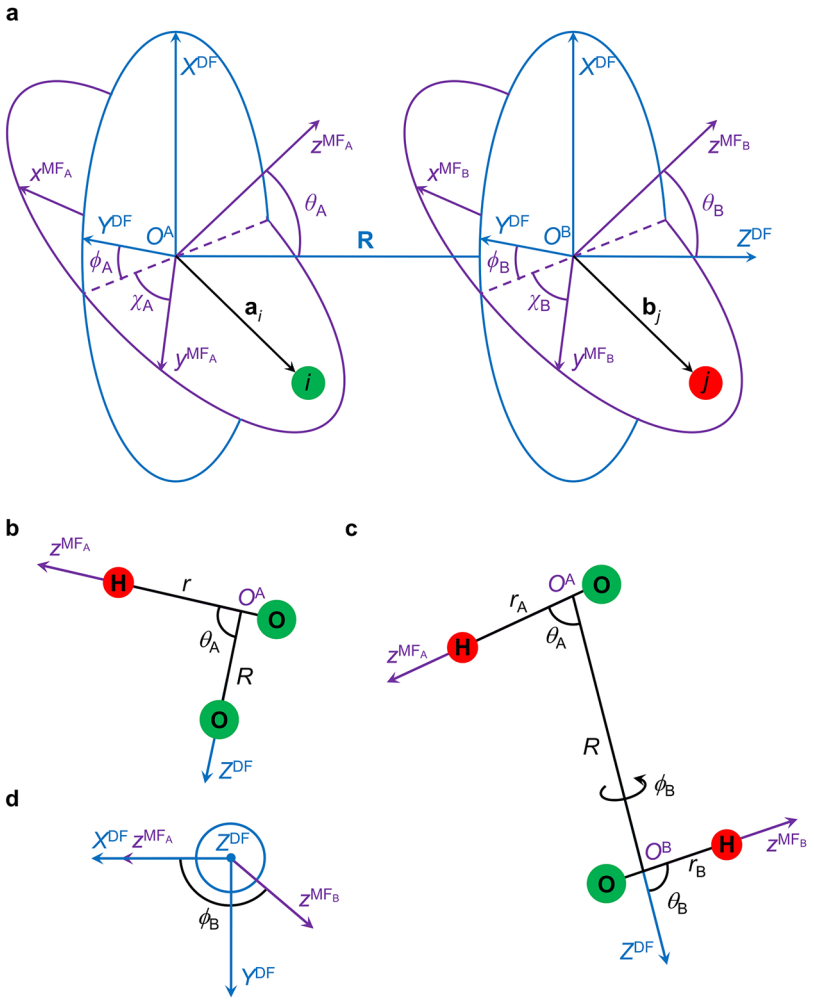

Figure 1. Coordinates employed for describing the configurations of the systems. (a) The coordinates of an arbitrary system. The axes of the DF and MF frames are labeled as (X^{DF}, Y^{DF}, Z^{DF}) and (x^{MF}, y^{MF}, z^{MF}), respectively. $\mathbf{a}_i$ and $\mathbf{b}_j$ denote the position vectors of the ith particle in monomer A and the jth particle in monomer B, respectively. (b) The coordinates for OH−O. (c) The coordinates for OH−OH. (d) Top view of the DF frame defined in (c), and thus ϕ_B is the angle between the projections of the z^{MF_A} and z^{MF_B} axes onto the XOY plane of the DF frame.

atom−diatom,[19,21,22,29−34] or diatom−diatom systems.[24,35−37] For instance, Spelsberg derived expressions for the long-range interaction of a monomer in a nondegenerate state with one with degeneracy, and applied them to construct the long-range IPES of the CO−OH system.[24] So far, no theory has been proposed to handle systems beyond atoms and linear molecules with degeneracy. This is because the degenerate states of linear molecules can be easily labeled by the projection of the electronic orbital angular momentum along the molecular axis, and then the expressions of the electrostatic properties (EPs) in the spherical tensor formalism can be simplified by using the angular momentum algebra. Obviously, there is a pressing need for a general method to formulate the long-range interaction of arbitrary two-body systems.

There are three main challenges in the development of a general method to calculate the long-range interaction energy. First, a general set of coordinates should be defined, which can describe the geometries of an arbitrary system, especially for polyatomic systems. Second, the derivation of the expressions of the specified system is often very tedious. Thus, a universal expression of the long-range interaction should be employed for developing a general method. Third, it must be able to handle molecules with various shapes, especially for the simplification of their EPs.

In this work, we focus on the general expression for the long-range IPES between two monomers with electronic degeneracy, derived using the degenerate perturbation theory of Schrödinger[19,24,38] with the multipole expansion of the Coulomb interaction Hamiltonian.[16,17,39,40] From the outset, we note that our discussion here neglects the spin−orbit coupling, but it can be easily incorporated into the same framework.[19,21,22,31] In addition, we introduce a group-theoretical method for determining the nonzero and independent EP components. This method is demonstrated in the construction of the long-range IPESs of the $O(^3P)$−$OH(^2\Pi)$ and $OH(^2\Pi)$−$OH(^2\Pi)$ systems, which are validated by comparing them to high-level *ab initio* points at selected geometries.

2. THEORY AND ALGORITHM

2.1. General Coordinates for Two-Body Systems

The basis of the general method for calculating the long-range interaction is the choice of the coordinates for describing the geometries of the system.[18] Here, a dimer-fixed (DF) frame $OXYZ$ is first defined as illustrated in Figure 1a, whose Z axis is fixed along the vector $\mathbf{R}$, with X and Y axes and origin arbitrarily

https://doi.org/10.1021/jacsau.5c00966
JACS Au 2025, 5, 5079−5088

chosen. O_A and O_B can be, for example, fixed at the center of mass of A and B, respectively. Second, the monomer-fixed frames attached to the monomers A and B (MF_Φ frame with Φ = A or B) are used to separate the intramolecular coordinates of the monomers and intermolecular coordinates, which must be invariant under the rotation or translation of the monomer Φ, such as the principal axes of the moment of inertia tensor of the monomer. The origin of the MF_Φ frame is fixed at O_Φ.

The intermolecular coordinates are chosen as $(R, \mathbf{\Omega}_A, \mathbf{\Omega}_B)$, in which $R \equiv |\mathbf{R}|$. $\mathbf{\Omega}_\Phi \equiv (\phi_\Phi, \theta_\Phi, \chi_\Phi)$ denotes the Euler angles specifying the orientation of the MF_Φ frame with respect to the DF frame.[41] Importantly, these coordinates are general for any molecular shape, while the intramolecular coordinates of A and B can be defined depending on how the vibrational coordinates are chosen. Note that for the systems including an atom or a linear molecule, not all the Euler angles are independent, as discussed in our previous study.[18] Two examples (the OH−O and OH−OH systems) are illustrated in Figure 1b−1d under such a general set of coordinates.

2.2. Long-Range Interaction of Two-Body Systems

Assuming two isolated monomers A and B are characterized by their respective Hamiltonian (H^A and H^B), perturbation theory can be used to determine the interaction energy in the long-range region, treating the interaction Hamiltonian V between two monomers as perturbation.[16,39] The starting point of the derivation for the expression of the long-range interaction is the multipole expansion of V in the spherical tensor form ($\hbar$ = 1)[16,39,40]

$$V = \sum_{l_1 l_2 m} (-1)^{l_2} \begin{pmatrix} 2l_1 + 2l_2 \\ 2l_1 \end{pmatrix}^{1/2} \langle l_1 m l_2 \bar{m} | (l_1 + l_2) 0 \rangle \times \frac{\hat{Q}^{A(DF)}_{l_1 m} \hat{Q}^{B(DF)}_{l_2 \bar{m}}}{R^{l_1+l_2+1}} \tag{1}$$

in which $(:)$ is the binomial coefficient, $\langle l_1 m l_2 \bar{m} | (l_1 + l_2) 0 \rangle$ is the Clebsch−Gordan coefficient, and $\bar{m} \equiv -m$. $\hat{Q}^{\Phi(DF)}_{lm}$ are the components of the 2^l-pole moment operator

$$\hat{Q}^{\Phi(DF)}_{lm} \equiv \sum_i e_i^\Phi r_i^l \sqrt{\frac{4\pi}{2l+1}} Y_l^m(\theta_i, \phi_i) \tag{2}$$

where these components are expressed in the DF frame. $\mathbf{r}_i = (r_i, \theta_i, \phi_i)$ is the position vector of the ith particle (electron or nucleus with the charge e_i^Φ) of Φ in the DF frame (fixed at the origin of the MF_Φ frame), with (θ_i, ϕ_i) as the polar and azimuthal angles. Y_l^m is the spherical harmonics. Then, the multipole moment operators in the DF frame are related to those in the MF_Φ frames by[40]

$$\hat{Q}^{\Phi(DF)}_{lm} = \sum_{m'} \hat{Q}^{(MF_\Phi)}_{lm'} D^{l*}_{mm'}(\phi_\Phi, \theta_\Phi, \chi_\Phi) \tag{3}$$

in which $D^l_{mm'}$ is the Wigner rotational matrix element.

If A and B are in $f_{A,\mu}$- and $f_{B,\nu}$-fold degenerate eigenstates $|\varphi^A_{\mu i}\rangle$ (i = 1, 2,⋯, $f_{A,\mu}$) and $|\varphi^B_{\nu k}\rangle$ (k = 1, 2,⋯, $f_{B,\nu}$) corresponding to the eigenenergies E^A_μ and E^B_ν of H^A and H^B, respectively, the unperturbed states, which can be chosen as products of the monomer eigenstates, e.g., $|\varphi^A_{\mu i}\varphi^B_{\nu k}\rangle \equiv |\varphi^A_{\mu i}\rangle\,|\varphi^B_{\nu k}\rangle$, define a diabatic potential energy matrix (DPEM) with the following elements indexed by ik and $i'k'$

$${}^{\mu\nu,ik,i'k'}E_{tot} \equiv E_{\mu\nu} + E^{(1)}_{\mu\nu,ik,i'k'} + E^{(2)}_{\mu\nu,ik,i'k'} \tag{4}$$

where $\mu\nu$ represents the unperturbed energy level with energy $E_{\mu\nu} \equiv E^A_\mu + E^B_\nu$. The first and second-order corrections are given by Schrödinger's degenerate perturbation theory[38,42]

$$E^{(1)}_{\mu\nu,ik,i'k'} = \langle \varphi^A_{\mu i}\varphi^B_{\nu k} | V | \varphi^A_{\mu i'}\varphi^B_{\nu k'} \rangle,$$

$$E^{(2)}_{\mu\nu,ik,i'k'} = -\sum_{nn' \neq \mu\nu} \frac{\langle \varphi^A_{\mu i}\varphi^B_{\nu k} | V | \varphi^A_n \varphi^B_{n'} \rangle \langle \varphi^A_n \varphi^B_{n'} | V | \varphi^A_{\mu i'}\varphi^B_{\nu k'} \rangle}{(E^A_n + E^B_{n'}) - (E^A_\mu + E^B_\nu)} \tag{5}$$

in which n and n' run over all unperturbed states except $n = \mu$ and $n' = \nu$. The long-range interaction energy ${}^{\mu\nu}E_{int}$ can be obtained by solving the following secular equation[19,24]

$$\det \left| ({}^{\mu\nu,ik,i'k'}E_{es} + {}^{\mu\nu,ik,i'k'}E^A_{ind} + {}^{\mu\nu,ik,i'k'}E^B_{ind} + {}^{\mu\nu,ik,i'k'}E_{disp}) - {}^{\mu\nu}E_{int}\delta_{ii'}\delta_{kk'} \right| = 0 \tag{6}$$

where $i, i' = 1, 2, \cdots, f_{A,\mu}$, and $k, k' = 1, 2, \cdots, f_{B,\nu}$. $\delta_{ii'}$ and $\delta_{kk'}$ are the Kronecker delta. ${}^{\mu\nu,ik,i'k'}E_{es}$, ${}^{\mu\nu,ik,i'k'}E^A_{ind}$, ${}^{\mu\nu,ik,i'k'}E^B_{ind}$, and ${}^{\mu\nu,ik,i'k'}E_{disp}$ are the electrostatic energy, the induction energy of the monomer A and B, and the dispersion energy expressed in the diabatic basis $|\varphi^A_{\mu i}\varphi^B_{\nu k}\rangle$, respectively

$${}^{\mu\nu,ik,i'k'}E_{es} \equiv \langle \varphi^A_{\mu i}\varphi^B_{\nu k} | V | \varphi^A_{\mu i'}\varphi^B_{\nu k'} \rangle,$$

$${}^{\mu\nu,ik,i'k'}E^A_{ind} \equiv -\sum_{k''} \sum_{n \neq \mu} [(E^A_n - E^A_\mu)^{-1} \langle \varphi^A_{\mu i}\varphi^B_{\nu k} | V | \varphi^A_n \varphi^B_{\nu k''} \rangle \times \langle \varphi^A_n \varphi^B_{\nu k''} | V | \varphi^A_{\mu i'}\varphi^B_{\nu k'} \rangle],$$

$${}^{\mu\nu,ik,i'k'}E^B_{ind} \equiv -\sum_{i''} \sum_{n' \neq \nu} [(E^B_{n'} - E^B_\nu)^{-1} \langle \varphi^A_{\mu i}\varphi^B_{\nu k} | V | \varphi^A_{\mu i''}\varphi^B_{n'} \rangle \times \langle \varphi^A_{\mu i''}\varphi^B_{n'} | V | \varphi^A_{\mu i'}\varphi^B_{\nu k'} \rangle],$$

$${}^{\mu\nu,ik,i'k'}E_{disp} \equiv -\sum_{n \neq \mu} \sum_{n' \neq \nu} [(E^A_n - E^A_\mu + E^B_{n'} - E^B_\nu)^{-1} \times \langle \varphi^A_{\mu i}\varphi^B_{\nu k} | V | \varphi^A_n \varphi^B_{n'} \rangle \langle \varphi^A_n \varphi^B_{n'} | V | \varphi^A_{\mu i'}\varphi^B_{\nu k'} \rangle] \tag{7}$$

Note that the third and higher order corrections of $E_{\mu\nu}$ are ignored in this work. This is reasonable because for neutral monomers, the leading term of the nth correction ($n > 1$) is proportional to R^{-3n}, which often is negligible when n is larger than 2.[16] Moreover, the above equations cannot be used for a system that has two identical monomers with $\mu \neq \nu$ due to existence of resonance interactions,[16] where the states $|\varphi^A_{\mu i}\rangle|\varphi^B_{\nu k}\rangle$, ($i$ = 1, 2,⋯, $f_{A,\mu}$, and k = 1, 2,⋯, $f_{B,\nu}$) and $|\varphi^A_{\nu k}\rangle|\varphi^B_{\mu i}\rangle$, ($k$ = 1, 2,⋯, $f_{A,\nu}$, and i = 1, 2,⋯, $f_{B,\mu}$) correspond to the same energy.

By substituting the multipole expansion of V into eq 7, each type of the interaction defined in the diabatic basis can be expressed in terms of R^{-n} for EP components, including multipole moments and (dynamic) polarizabilities, whose explicit form is given in Section S−I of Supporting Information (SI). By employing the relationship between the components of the multipole moment operators of Φ expressed in the MF_Φ and DF frames, the EP components can be expressed in the MF_Φ frame, which depend solely on its intramolecular coordinates and are related to those in the DF frame by the transformation from the MF_Φ to DF frame. Consequently, we only need to deal with these components in the MF_Φ frame, which can be determined using *ab initio* calculations of the monomers, such as the finite field method (FFM).[43] The formulas of the long-range

https://doi.org/10.1021/jacsau.5c00966
JACS Au 2025, 5, 5079−5088

interaction in the Cartesian form are also derived in this work and given in Section S−I of SI.

2.3. Independent Components of EPs

It is important to sort out the nonzero and independent components of monomer EPs not only for calculation efficiency, but also to avoid inaccuracies inherent in *ab initio* calculations. The latter is known to contort the relationship between the nonzero EP components, leading to inaccurate results, especially for monomers in degenerate states. This can be achieved using a group-theoretical method.[18,40] Since degenerate states do not transform with the totally symmetric irreducible representation of the monomer point group, the symmetry properties of both the multipole moment operators and the degenerate states need to be carefully considered. As mentioned in Section 1, the nonzero EP components of an atom or a linear molecule have been derived by previous studies,[19,24,32] so in this work, we mainly focus on nonlinear molecules. A brief derivation of the results of the atoms and linear molecules with the $C_{\infty v}$ or $D_{\infty h}$ symmetry can be found in Section S−II in SI.

The point group of a nonlinear molecule is finite. So, it is convenient to employ the projection operator of the corresponding irreducible representation to derive the nonzero EP components and their relationship, including the 2^l-pole moment ${}^{\mu,ii'}Q_{lm}$ and the 2^l-pole−$2^{l'}$-pole dynamic polarizability ${}^{\mu,ii'}\alpha_{lm,l'm'}(i\omega)$ defined as follows

$$
\begin{aligned}
{}^{\mu,ii'}Q_{lm} &= \langle \varphi_{\mu i}|\hat{Q}_{lm}|\varphi_{\mu i'}\rangle,\\
{}^{\mu,ii'}\alpha_{lm,l'm'}(i\omega) &= \sum_{n\neq\mu}\{(E_n - E_\mu)[(E_n - E_\mu)^2 + \omega^2]^{-1}\\
&\quad \times 2\langle \varphi_{\mu i}|\hat{Q}_{lm}|\varphi_n\rangle\langle \varphi_n|\hat{Q}_{l'm'}|\varphi_{\mu i'}\rangle\}
\end{aligned}
\tag{8}
$$

in which i is the imaginary unit, ω is the angular frequency. First, for the multipole moment operator $\hat{Q}_{lm}$, its transformations under symmetry operations of the monomer's point group are the same as Y_l^m, in which the representation matrices of the latter have been realized for many common-used finite groups by the GTPack package.[44,45] For degenerate states that transform according to two- or higher-dimensional irreducible representations of the molecular point group, because two sets of states of the same degenerate energy level are related by a unitary matrix, and these different definitions have no influence on the eigenvalues of the DPEM, we only need to derive the transformations of the degenerate states in a specified definition under the symmetry operations. In this work, we employed the Cornwell method, which is based on the real-valued Cartesian tesseral harmonics, implemented in GTPack to obtain the representation matrices of a degenerate state. Third, for the 2^l-pole−$2^{l'}$-pole polarizability with $l = l'$, an additional permutation symmetry between two multipole moment operators makes ${}^{\mu,ii}\alpha_{lm,lm'}(i\omega)$ equal to ${}^{\mu,ii}\alpha_{lm',lm}(i\omega)$ when $|\varphi_{\mu i}\rangle$ is chosen as real-valued function. This property further reduces the number of independent components of polarizability.

Based on the above strategy, we develop the Mathematica programs for determining the nonzero EP components and their relationships. The derivations of the expressions employed in this program are provided in Section S−III in SI. In practical applications, the value of these quantities can be determined by FFM.[43] The advantage of FFM is that it is based on the change of the energy of the molecule under an external field. Thus, we do not need to know the explicit form of the degenerate states of the molecule. For the EP components defined as eq 8 with $i = i'$, the symmetry breaking of the degeneracy under an external field can be analyzed from the output files of the *ab initio* package. Then, the components with $i \neq i'$ related to those with $i = i'$ can be obtained.

2.4. Algorithm

For the general method for calculating the long-range interaction energy developed in this work, the following workflow was established, as illustrated in Figure 2. First, the

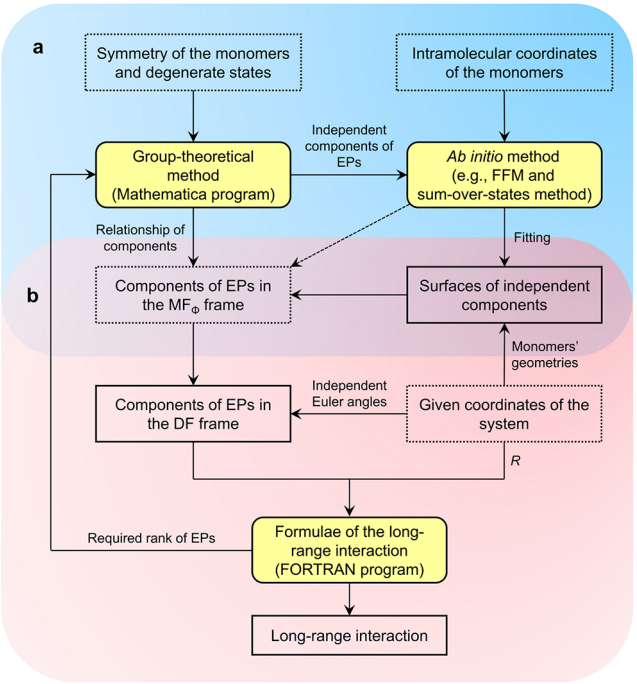

Figure 2. Workflow for calculating the long-range interaction for a given structure of the system, which consists of two steps. (a) The derivation, calculation, and fitting of the independent EP components in the MF frame of the monomers. The dashed arrow from "*Ab initio* method" to "Components of EPs in the MF$_\Phi$ frame" denotes the direct calculation of these quantities. (b) The calculation of the long-range interaction energy. The quantities with the dashed border represent the input data of each step.

MF$_\Phi$ frame is chosen to be consistent with the coordinate system defined in the GTpack package for the point group of the monomer Φ, and then the Mathematica programs provided in the SI are used to derive all the nonzero EP components up to the required rank and their relationships. Next, an *ab initio* method, e.g., the FFM, is employed to calculate the independent EP components, and then these *ab initio* data are fitted as functions of the intramolecular coordinates. After all EP components in the MF$_\Phi$ frame are determined for a given configuration of the monomers, they are used to express all EP components in the DF frame by employing the relationships between them, as illustrated by eqs (S11) to (S13), (S25), and (S26). Finally, substituting these EP components into eq 7, the long-range interaction can be obtained by solving eq 6 as a function of R.

https://doi.org/10.1021/jacsau.5c00966
JACS Au 2025, 5, 5079−5088

3. COMPUTATIONAL DETAILS

3.1. Formulas of IPESs of O(^{3}P)−OH($^2\Pi$) and OH($^2\Pi$)−OH($^2\Pi$)

To illustrate our method, the long-range IPESs of the O(^{3}P)−OH($^2\Pi$) and OH($^2\Pi$)−OH($^2\Pi$) systems were constructed as examples. The former is an important atmospheric and astrochemical reaction and served as a prototype for investigating geometric phase effects in chemical reactions,[46−48] while the latter is crucial for studying collisional dynamics under an external electric or magnetic field.[49−51] Although many PESs have been reported,[20,52−65] the long-range IPESs for these systems have seldom been addressed with the degeneracy considered.[21,22]

We employed the expressions of the long-range interaction energy in either the Cartesian or spherical tensor form to construct the long-range IPESs of the O(^{3}P)−OH($^2\Pi$) and OH($^2\Pi$)−OH($^2\Pi$) systems, whenever the form is the most convenient. If, for example, the spin−orbit coupling of these two systems were to be included, expressions in the spherical tensor form are preferred to take advantage of angular momentum algebra.[19] Moreover, because the long-range interaction calculated by these two forms should be identical, we can use this property to check the accuracy of these two programs. In this work, to improve the accuracy of the IPESs, the calculation of the dispersion interaction employed the expression derived by the Casimir−Polder integral transformation,[66,67] which requires the explicit form of dynamic polarizabilities of the monomers as a function of ω.

For OH($^2\Pi$, A)−O(^{3}P, B), the electrostatic energy with the terms proportional to R^{-4}, R^{-5}, and R^{-6}, the induction energy of O with the terms proportional to R^{-6} and R^{-7}, and the dispersion energy with the terms proportional to R^{-6} and R^{-7}, expressed in the spherical tensor form with the diabatic basis $|\kappa\Lambda\rangle|\eta 1 M_L\rangle$ ($\Lambda = \pm 1$, $M_L = 0, \pm 1$), and in the Cartesian form with the diabatic basis $|\kappa 1,i\rangle|\eta 1,k\rangle$ ($i = x, y, k = a, b, c$) were used. The definitions of these diabatic basis are given in Section S−II in SI. The leading term of the induction energy of OH is proportional to R^{-8}, thus, we neglected this interaction.

For OH($^2\Pi$, A)−OH($^2\Pi$, B), the electrostatic energy with the terms proportional to R^{-3}, R^{-4}, and R^{-5}, the induction energy of the monomers A and B with the terms proportional to R^{-6} and R^{-7}, and the dispersion energy with the terms proportional to R^{-6} and R^{-7}, expressed in the spherical tensor form with the diabatic basis $|\kappa\Lambda\rangle|\kappa'\Lambda'\rangle$ ($\Lambda = \pm 1$, $\Lambda' = \pm 1$), and in the Cartesian form with the diabatic basis $|\kappa 1,i\rangle|\kappa' 1,k\rangle$ ($i = x, y, k = x, y$) were used.

In both cases, identical long-range IPESs were obtained in the spherical tensor and Cartesian forms, validating the derivations.

3.2. *Ab Initio* Calculations

The independent EP components of the O(^{3}P) atom and the OH($^2\Pi$) radical in their MF frames were calculated by employing FFM,[43] in which the states and multipole moment operators are expressed in the Cartesian form, see Sections S−I and S−II in SI for details. The independent quantities were fitted as functions of the O−H bond length, ranging from 1.5 to 3.0 a_0, using the cubic spline interpolation.

Ab initio calculations of the multipole moments and the static polarizabilities were performed in the MOLPRO 2015 package[68,69] by the internally contracted multireference configuration interaction (icMRCI) method[70,71] with the augmented correlation-consistent polarized valence quintuple-ζ (AV5Z)[72] basis set. Completed active space self-consistent field (CASSCF) wave functions[73,74] were calculated first, and their natural orbitals were used in the MRCI calculations. For O(^{3}P), 6 electrons and 4 active orbitals were included in the active space, while 5 electrons and 4 active orbitals were used for OH($^2\Pi$). These *ab initio* calculations were performed in C_1 symmetry. The magnitudes of the external field E_α and gradients $E_{\alpha\beta}$ and $E_{\alpha\beta\gamma}$ used in calculating these quantities are listed in Table S1 in SI. Other EPs of these two monomers are determined by using the relationship between nonzero components. The independent EP components of the O(^{3}P) atom and the OH($^2\Pi$) radical defined in the spherical tensor form were determined by employing the relationship between the EP components in the Cartesian and spherical tensor forms given in Section S−IV in SI, while the values of these Cartesian components are given in Section S−V in SI (Table S2, Figures S1 and S2). Calculating the components of the dynamic polarizabilities as functions of ω by the Padé approximation requires the corresponding Cauchy moments $c_{p,k}$ defined as follows[75]

$$\alpha_p(\mathrm{i}\omega) = \sum_{k=0}^{\infty} c_{p,k}(-\omega^2)^k \tag{9}$$

where p denotes the component of the polarizability. In this work, the Dalton2024.0-dev package was used to obtain these quantities at the CASSCF/AV5Z level by linear response calculations.[76,77] For O(^{3}P), 8 electrons and 15 (62212110) active orbitals were included in the active space with the *ab initio* calculation under the D_{2h} symmetry, while for OH($^2\Pi$), 9 electrons and 10 (6220) active orbitals were included in the active space with the *ab initio* calculation under the C_{2v} symmetry. The max value of k in eq 9 was chosen as 19. Then, the $[n - 1/n]$ Padé approximation[39,75] with $n = 9$ was employed to obtain the explicit form of the components of the dynamic polarizabilities as a function of ω. Similar to the discussion of the static polarizabilities, only the Cauchy moments with $i = i'$ were calculated, while other components are determined by using the relationship between nonzero components. Then, these components can also be transformed between the Cartesian and spherical tensor form by the relationships given in Section S−IV in SI. The Cauchy moments with $k = 0$, which are the components of the static polarizability, are compared with those obtained by FFM in Table S2 and Figure S3 in the SI, to illustrate the validity of the setting of the *ab initio* parameters.

The integrals of the product of these components of the dynamic polarizabilities of A and B over ω were calculated by the trapezoidal rule. ω is in the range from 0 to 50 au, while $\Delta\omega$ = 0.01 au. These quantities were found to be converged within 1%, and then fitted by $\sum_{t=0}^{4} w_{1,t} r^t$ for O−OH and $\sum_{t+t'=0}^{3} w_{2,tt'} r_A^t r_B^{t'}$ for OH−OH with r, r_A, and r_B in the range from 1.5 to 3.0 a_0.

In order to test the accuracy of the long-range IPESs of the O(^{3}P)−OH($^2\Pi$) and OH($^2\Pi$)−OH($^2\Pi$) systems, high-level *ab initio* calculations of the interaction energies of these two systems were also performed, which are defined as

$$E_{\mathrm{int}} = E_{\mathrm{tot}} - E_{\mathrm{tot},\infty} \tag{10}$$

where E_{int} and E_{tot} are the interaction energy and total energy of the corresponding structure of the system, respectively. $E_{\mathrm{tot},\infty}$ is the total energy of the system where the distance between two monomers is infinite, and thus their interaction vanishes. The geometry with r = 1.83 a_0, R = 100 a_0, and $\theta_A = 0°$ of the O−OH system, and the geometry of the OH−OH system with $r_A = r_B$ =

https://doi.org/10.1021/jacsau.5c00966
JACS Au 2025, 5, 5079−5088

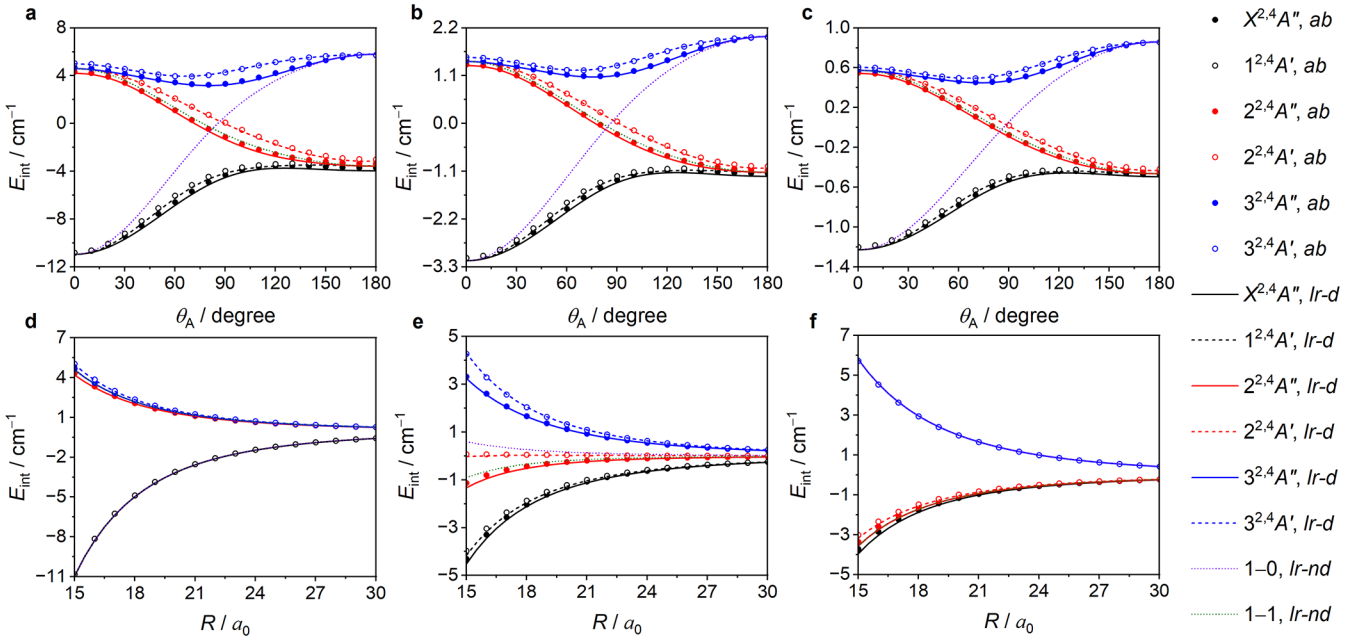

Figure 3. Interaction energies of the O(^{3}P)−OH($^2\Pi$) system with the OH bond length (r) fixed at 1.83 a_0. (a−c) Interaction energies as a function of θ_A with R = (a) 15, (b) 20, and (c) 25 a_0. (d−f) Interaction energies as a function of R with θ_A = (d) 0°, (e) 90°, and (f) 180°. In both panels, *ab* and *lr-d* denote the *ab initio* results and the multipolar interaction energies derived from degenerate perturbation theory, respectively. Λ-M_L, *lr-nd* denotes the interaction energy between the OH radical in the $|\kappa\Lambda\rangle$ state and the O atom in the $|\eta 1 M_L\rangle$ state obtained by the nondegenerate perturbation theory. Since the latter are independent of the sign of Λ and M_L, only the 1−0, *lr-nd* and 1−1, *lr-nd* results are included.

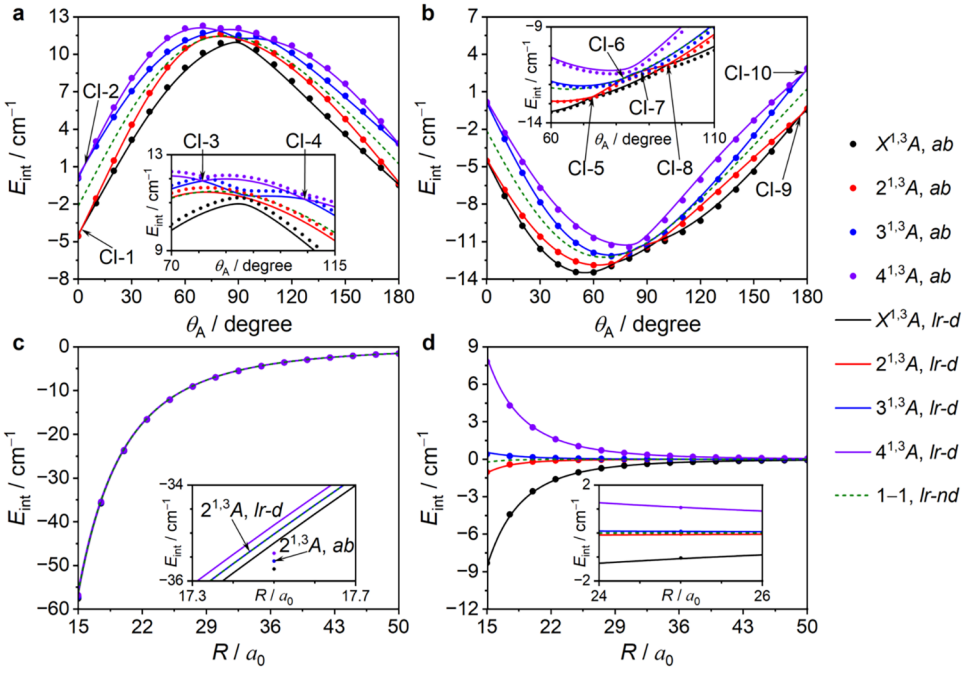

Figure 4. Interaction energies of the OH($^2\Pi$)−OH($^2\Pi$) system with $r_A = r_B$ = 1.83 a_0. (a) Interaction energies as a function of θ_A with R = 20 a_0, ϕ_B = 0°, and θ_B = 90°. (b) Interaction energies as a function of θ_A with R = 20 a_0, ϕ_B = 180°, and θ_B = 90°. (c) Interaction energies as a function of R with $\theta_A = \phi_B = \theta_B$ = 0°. (d) Interaction energies as a function of R with $\theta_A = \phi_B = \theta_B$ = 90°. In all panels, *ab* and *lr-d* denote the *ab initio* results and the multipolar interaction energies, respectively. *i-k*, *lr-nd* denotes the interaction energy between OH in the $|\kappa i\rangle$ and $|\kappa k\rangle$ (i, k = 1, −1) states obtained by the nondegenerate perturbation theory. Since the latter are independent of the sign of Λ and Λ′, only the curve 1−1, *lr-nd* is included. The positions of CIs labeled as CI-1 to CI-10 are marked with arrows in (a, b).

1.83 a_0, R = 400 a_0, and $\theta_A = \phi_B = \theta_B$ = 0° were chosen to calculate $E_{tot,\infty}$ of these systems. The total energy of the O(^{3}P)−OH($^2\Pi$) system was calculated at the icMRCI[70,71]/AV5Z[72] level by the MOLPRO package, while 9 electrons and 7 active orbitals were included in the active space. These *ab initio* calculations were performed in C_1 symmetry. For the total energy of OH($^2\Pi$)−OH($^2\Pi$), the *ab initio* calculations were performed in the C_1 symmetry at the icMRCI[70,71]/AV5Z[72] level, where 10 electrons and 8 active orbitals were included in the active space.

https://doi.org/10.1021/jacsau.5c00966
JACS Au 2025, 5, 5079−5088

4. RESULTS AND DISCUSSION

4.1. Long-Range IPES of O(^{3}P)−OH($^2\Pi$)

There are six pairs of states correlated to the O(^{3}P)−OH($^2\Pi$) asymptote, denoted as $X^{2,4}A''$, $1^{2,4}A'$, $2^{2,4}A''$, $2^{2,4}A'$, $3^{2,4}A''$, and $3^{2,4}A'$. The doublets and quartets have the same total energies due to the neglect of the spin−orbit coupling. At $\theta_A = 0°$, the states can be assigned as $^{2,4}\Pi$, $^{2,4}\Sigma^-$, $^{2,4}\Delta$, and $^{2,4}\Sigma^+$ with increasing energy. However, at $\theta_A = 180°$, these states are $^{2,4}\Sigma^-$, $^{2,4}\Delta$, $^{2,4}\Sigma^+$, and $^{2,4}\Pi$. The change of energy order at the two collinear geometries (OHO vs OOH) underscores the nonadiabatic interaction among these states. We emphasize that the assignment of these adiabatic states differs from the previous work on the C(^{3}P)−OH($^2\Pi$) and Si(^{3}P)−OH($^2\Pi$) systems,[19,31] because the electron configurations of the O and C (or Si) atoms are $1s^22s^22p^4$ and $1s^22s^22p^2$ (or $1s^22s^22p^63s^23p^2$) event though both are in a ^{3}P state.

Figure 3 compares the multipolar and *ab initio* interaction energies as a function of θ_A (Figure 3a−3c) and R (Figure 3d−3f). The excellent agreement confirms the accuracy of these long-range IPESs. For comparison, the interaction energies calculated using the nondegenerate perturbation theory, namely the diagonal elements of the DPEM (excluding energies of two monomers), are also included in the figure as Λ−M_L, *lr-nd*, which are obviously in error, due to neglect of nonadiabatic effects. As shown in Figure S4 in Section S−VI in SI, our method starts to deviate from *ab initio* data when R is less than 10 a_0.

4.2. Long-Range IPES of OH($^2\Pi$)−OH($^2\Pi$)

We now turn to the long-range IPESs for the first four state pairs of the OH($^2\Pi$)−OH($^2\Pi$) system, denoted as $X^{1,3}A$, $2^{1,3}A$, $3^{1,3}A$, and $4^{1,3}A$. In Figure 4, the multipolar interaction energies and their dependence on θ_A (a, b) and R (c, d) are compared with *ab initio* results, and the excellent agreement validates again the accuracy of our approach. To highlight the inadequacy of the nondegenerate theory, some results are also included in the figure for comparison. Similar to the O(^{3}P)−OH($^2\Pi$) system, the comparison between the multipolar and *ab initio* interaction energies in the short-range region, as plotted in Figure S5 in Section S−VI in SI, also shows that our method is accurate with R larger than 10 a_0.

Compared with the O(^{3}P)−OH($^2\Pi$) system, the lower C_1 symmetry of the system allows the formation of conical intersections (CIs), as shown by arrows in Figure 4a,b. As shown in Figure 4a, one can find four CIs with $\phi_B = 0°$, which are between the $X^{1,3}A$ and $2^{1,3}A$ states with $\theta_A = 1.71°$, and the $3^{1,3}A$ and $4^{1,3}A$ states with $\theta_A = 3.87$, 78.53, and 106.66°. For Figure 4b, there are six CIs when $\phi_B = 180°$, which are between the $X^{1,3}A$, and $2^{1,3}A$ states with $\theta_A = 72.66$, 95.73, and 176.11°, the $2^{1,3}A$ and $3^{1,3}A$ states with $\theta_A = 82.15$ and 87.63°, and the $3^{1,3}A$ and $4^{1,3}A$ states with $\theta_A = 178.28°$. These CIs are confirmed by the fact that line integrals around the above CIs are equal to π, as shown in Figures S6 and S7 in Section S−VII in SI. These CIs result in complicated behavior of these IPESs, which would make the fitting of the adiabatic interaction energies quite difficult,[78] underscoring the advantages of the degenerate perturbation approach. Moreover, these CIs are along the coordinate θ_A, thus it would be interesting to study the effect of these CIs on the stereodynamics in (ultra)cold collisions between the OH($^2\Pi$) dimer.

Interestingly, the leading electrostatic term of this system is the dipole−dipole interaction. Indeed, the IPESs are approximately proportional to sin θ_A in Figure 4a and −sin θ_A in Figure 4b. Note that since the dipole−dipole term has no contribution to the off-diagonal elements of the DPEM, however, the splitting of the four electronic states becomes visible only when the dipole−dipole electrostatic interaction is relatively small. Indeed, the four pairs of states have almost no difference when the dipole−dipole interaction is the maximum, while they diverge in Figure 4d when the dipole−dipole interaction is zero.

5. CONCLUSIONS

In this work, we have developed a general framework for characterizing the long-range interaction energy between two monomers with electronic degeneracy by employing the degenerate perturbation theory of Schrödinger. First, we presented the electrostatic, induction, and dispersion energy terms as the multipole expansion of the Coulomb interaction Hamiltonian. Then, a group-theoretical method was developed to determine the nonzero components of the EPs of monomers and their relationships. By calculating these independent quantities and fitting them as functions of monomer intramolecular coordinates, the long-range interaction between monomers can be calculated following the same workflow of our recently developed program ABLRI.[18] To validate the accuracy of this method, we constructed the IPESs of the O(^{3}P)−OH($^2\Pi$) and OH($^2\Pi$)−OH($^2\Pi$) systems and compared them to high-level *ab initio* results. The method performed remarkably well, especially reproducing the long-range behavior impacted by the breakdown of the BOA. This method thus lays a solid foundation for accurate dynamical calculations of systems containing monomers with electronic degeneracy at low temperatures.

■ ASSOCIATED CONTENT

Supporting Information

The Supporting Information is available free of charge at https://pubs.acs.org/doi/10.1021/jacsau.5c00966.

The programs of the long-range IPESs of the O(^{3}P)−OH($^2\Pi$) and OH($^2\Pi$)−OH($^2\Pi$) systems; the Mathematica programs for the derivation of the non-zero components of the EPs and their relationships (ZIP)

Details of the expressions and derivations; independent EP components of OH($^2\Pi$) and O(^{3}P) and comparison of these components obtained by different methods; interaction energies of the O(^{3}P)−OH($^2\Pi$) and OH($^2\Pi$)−OH($^2\Pi$) systems as a function of R in the short-range region; the magnitudes of the external field and gradients when calculating the independent EP components of monomers O(^{3}P) and OH($^2\Pi$); the derivative coupling and the line integral along the small circle around the CI-1 to CI-10 (PDF)

■ AUTHOR INFORMATION

Corresponding Authors

Xixi Hu − *Kuang Yaming Honors School, Institute for Brain Sciences, Jiangsu Key Laboratory of Vehicle Emissions Control, Center of Modern Analysis, Nanjing University, Nanjing, Jiangsu 210023, China; Hefei National Laboratory, Hefei, Anhui 230088, China;* orcid.org/0000-0003-1530-3015; Email: xxhu@nju.edu.cn

Hua Guo − *Department of Chemistry and Chemical Biology, Center for Computational Chemistry, University of New Mexico, Albuquerque, New Mexico 87131, United States;*

https://doi.org/10.1021/jacsau.5c00966
JACS Au 2025, 5, 5079−5088

orcid.org/0000-0001-9901-053X; Email: hguo@unm.edu

Daiqian Xie − *State Key Laboratory of Coordination Chemistry, Key Laboratory of Mesoscopic Chemistry of MOE, School of Chemistry and Chemical Engineering, Nanjing University, Nanjing 210023, China; Hefei National Laboratory, Hefei, Anhui 230088, China;* orcid.org/0000-0001-7185-7085; Email: dqxie@nju.edu.cn

Author

Yipeng Yu − *State Key Laboratory of Coordination Chemistry, Key Laboratory of Mesoscopic Chemistry of MOE, School of Chemistry and Chemical Engineering, Nanjing University, Nanjing 210023, China*

Complete contact information is available at: https://pubs.acs.org/10.1021/jacsau.5c00966

Author Contributions

Y.Y., X.H., H.G., and D.X. conceived the research. Y.Y. derived the expressions and wrote the programs. The manuscript was written through the contributions of all authors. All authors have given approval to the final version of the manuscript. X.H., H.G., and D.X. supervised the study and provided the funding.

Funding

D.X. is supported by the National Natural Science Foundation of China (Grant Nos. 22233003 and 22241302) and the Innovation Program for Quantum Science and Technology (2021ZD0303305). X.H. is supported by the National Natural Science Foundation of China (22473057) and the AI & AI for Science Project of Nanjing University (14380023). H.G. is supported by US Department of Energy (DE-SC0015997).

Notes

The authors declare no competing financial interest.

■ ACKNOWLEDGMENTS

We are grateful to the High-Performance Computing Center (HPCC) of Nanjing University.

■ REFERENCES

(1) Quéméner, G.; Julienne, P. S. Ultracold molecules under control! *Chem. Rev.* **2012**, *112* (9), 4949−5011.
(2) Stuhl, B. K.; Hummon, M. T.; Ye, J. Cold state-selected molecular collisions and reactions. *Annu. Rev. Phys. Chem.* **2014**, *65*, 501−518.
(3) Liu, Y.; Ni, K.-K. Bimolecular chemistry in the ultracold regime. *Annu. Rev. Phys. Chem.* **2022**, *73*, 73−96.
(4) Krems, R. V. *Molecules in Electromagnetic Fields*; Wiley: Hoboken, NJ, 2018.
(5) Balakrishnan, N. Perspective: Ultracold molecules and the dawn of cold controlled chemistry. *J. Chem. Phys.* **2016**, *145* (15), No. 150901.
(6) Krems, R. V. Cold controlled chemistry. *Phys. Chem. Chem. Phys.* **2008**, *10* (28), 4079−4092.
(7) Hutson, J. M. Theory of Cold Atomic and Molecular Collisions. In *Cold Molecules: Theory, Experiment, Applications*, 1st ed.; Krems, R. V.; Stwalley, W. C.; Friedrich, B., Eds.; CRC Press: Boca Raton, 2009; pp 3−38.
(8) Liu, Y.; Luo, L. Molecular collisions: From near-cold to ultra-cold. *Front. Phys.* **2021**, *16* (4), No. 42300.
(9) Bell, M. T.; Softley, T. P. Ultracold molecules and ultracold chemistry. *Mol. Phys.* **2009**, *107* (2), 99−132.
(10) Lemeshko, M.; Krems, R. V.; Doyle, J. M.; Kais, S. Manipulation of molecules with electromagnetic fields. *Mol. Phys.* **2013**, *111* (12−13), 1648−1682.
(11) Weck, P. F.; Balakrishnan, N. Importance of long-range interactions in chemical reactions at cold and ultracold temperatures. *Int. Rev. Phys. Chem.* **2006**, *25* (3), 283−311.
(12) Ospelkaus, S.; Ni, K. K.; Wang, D.; de Miranda, M. H. G.; Neyenhuis, B.; Quemener, G.; Julienne, P. S.; Bohn, J. L.; Jin, D. S.; Ye, J. Quantum-state controlled chemical reactions of ultracold potassium-rubidium molecules. *Science* **2010**, *327* (5967), 853−857.
(13) Liu, Y.; Hu, M.-G.; Nichols, M. A.; Yang, D.; Xie, D.; Guo, H.; Ni, K.-K. Precision test of statistical dynamics with state-to-state ultracold chemistry. *Nature* **2021**, *593* (7859), 379−384.
(14) Jiang, B.; Cheng, C.; Yang, D.; Guo, H.; Xie, D.; Shen, X. Dynamics of collision-induced energy transfer. *Fundam. Res.* **2023** DOI: 10.1016/j.fmre.2023.09.010.
(15) Ahlrichs, R. Convergence properties of the intermolecular force series (1/*R*-expansion). *Theor. Chim. Acta* **1976**, *41* (1), 7−15.
(16) Stone, A. J. *The Theory of Intermolecular Forces*, 2nd ed.; Oxford University Press: Oxford, 2013.
(17) Buckingham, A. D.; Fowler, P. W.; Hutson, J. M. Theoretical studies of van der Waals molecules and intermolecular forces. *Chem. Rev.* **1988**, *88* (6), 963−988.
(18) Yu, Y.; Yang, D.; Hu, X.; Xie, D. ABLRI: A program for calculating the long-range interaction energy between two monomers in their non-degenerate states. *J. Chem. Phys.* **2024**, *160* (17), No. 172501.
(19) Bussery-Honvault, B.; Dayou, F.; Zanchet, A. Long-range multipolar potentials of the 18 spin-orbit states arising from the $C(^3P)$ + $OH(X^2\Pi)$ interaction. *J. Chem. Phys.* **2008**, *129* (23), No. 234302.
(20) Kendrick, B.; Pack, R. T. Potential energy surfaces for the low-lying $^2A''$ and $^2A'$ States of HO_2: Use of the diatomics in molecules model to fit *ab initio* data. *J. Chem. Phys.* **1995**, *102* (5), 1994−2012.
(21) Graff, M. M.; Wagner, A. F. Theoretical studies of fine-structure effects and long-range forces: Approximating the reactive surface of $O(^3P)$ + $OH(^2\Pi)$. *Chem. Phys. Lett.* **1990**, *174* (3), 287−293.
(22) Graff, M. M.; Wagner, A. F. Theoretical studies of fine-structure effects and long-range forces: Potential-energy surfaces and reactivity of $O(^3P)$ + $OH(^2\Pi)$. *J. Chem. Phys.* **1990**, *92* (4), 2423−2439.
(23) Gentry, W. R.; Giese, C. F. Long-range interactions of ions with atoms having partially filled p subshells. *J. Chem. Phys.* **1977**, *67* (5), 2355−2361.
(24) Spelsberg, D. Dynamic multipole polarizabilities and reduced spectra for OH, application to the long-range part of the two lowest potential surfaces of the OH−CO complex. *J. Chem. Phys.* **1999**, *111* (21), 9625−9633.
(25) Bettens, R. P. A.; Collins, M. A. Multiple surface long-range interaction potentials between $C(^3P_j)$ and closed-shell molecules. *J. Chem. Phys.* **2002**, *116* (1), 101−104.
(26) Krems, R. V.; Groenenboom, G. C.; Dalgarno, A. Electronic interaction anisotropy between atoms in arbitrary angular momentum states. *J. Phys. Chem. A* **2004**, *108* (41), 8941−8948.
(27) Flannery, M. R.; Vrinceanu, D.; Ostrovsky, V. N. Long-range interaction between polar Rydberg atoms. *J. Phys. B:At., Mol. Opt. Phys.* **2005**, *38* (2), No. S279.
(28) Groenenboom, G. C.; Chu, X.; Krems, R. V. Electronic anisotropy between open shell atoms in first and second order perturbation theory. *J. Chem. Phys.* **2007**, *126* (20), No. 204306.
(29) Nielson, G. C.; Parker, G. A.; Pack, R. T. van der Waals interactions of Π-state linear molecules with atoms. C_6 for $NO(X\ ^2\Pi)$ interactions. *J. Chem. Phys.* **1976**, *64* (5), 2055−2061.
(30) Lepers, M.; Dulieu, O. Cold atom-molecule photoassociation: long-range interactions beyond the $1/R^n$ expansion. *Eur. Phys. J. D* **2011**, *65* (1), 113−123.
(31) Bussery-Honvault, B.; Dayou, F. $Si(^3P)$ + $OH(X^2\Pi)$ interaction: Long-range multipolar potentials of the eighteen spin−orbit states. *J. Phys. Chem. A* **2009**, *113* (52), 14961−14968.
(32) Skomorowski, W.; Moszynski, R. Long-range interactions between an atom in its ground S state and an open-shell linear molecule. *J. Chem. Phys.* **2011**, *134* (12), No. 124117.

(33) Lepers, M.; Bussery-Honvault, B.; Dulieu, O. Long-range interactions in the ozone molecule: Spectroscopic and dynamical points of view. *J. Chem. Phys.* **2012**, *137* (23), No. 234305.
(34) Stoecklin, T.; Bussery-Honvault, B.; Honvault, P.; Dayou, F. Asymptotic potentials and rate constants in the adiabatic capture centrifugal sudden approximation for X+OH($X^2\Pi$)→OX+H(^{2}S) reactions where X = O(^{3}P), S(^{3}P) or N(^{4}S). *Comput. Theor. Chem.* **2012**, *990*, 39−46.
(35) Wormer, P. E. S.; Kłos, J. A.; Groenenboom, G. C.; van der Avoird, A. *Ab initio* computed diabatic potential energy surfaces of OH−HCl. *J. Chem. Phys.* **2005**, *122* (24), No. 244325.
(36) Kirste, M.; Wang, X.; Schewe, H. C.; Meijer, G.; Liu, K.; van der Avoird, A.; Janssen, L. M. C.; Gubbels, K. B.; Groenenboom, G. C.; van de Meerakker, S. Y. T. Quantum-state resolved bimolecular collisions of velocity-controlled OH with NO radicals. *Science* **2012**, *338* (6110), 1060−1063.
(37) Karman, T.; Besemer, M.; van der Avoird, A.; Groenenboom, G. C. Diabatic states, nonadiabatic coupling, and the counterpoise procedure for weakly interacting open-shell molecules. *J. Chem. Phys.* **2018**, *148* (9), No. 094105.
(38) Landau, L. D.; Lifshitz, E. M. Perturbation Theory. In *Quantum Mechanics: Non-Relativistic Theory*, 3rd ed.; Pergamon Press: Oxford, 1977; pp 133−163.
(39) Kaplan, I. G. *Intermolecular Interactions: Physical Picture, Computational Methods and Model Potentials*; John Wiley & Sons, Inc.: Chichester, England, 2006.
(40) Leavitt, R. P. An irreducible tensor method of deriving the long-range anisotropic interactions between molecules of arbitrary symmetry. *J. Chem. Phys.* **1980**, *72* (6), 3472−3482.
(41) Zare, R. N. *Angular Momentum: Understanding Spatial Aspects in Chemistry and Physics*; John Wiley & Sons, Inc.: New York, 1988.
(42) Dmitriev, Y. Adiabatic perturbation theory for the degenerate case. I. Perturbation of isolated degenerate or quasidegenerate levels. *Int. J. Quantum Chem.* **1975**, *9* (6), 1033−1045.
(43) Chen, H.; Liu, M.; Yan, T. Molecular multipoles and (hyper)polarizabilities of water by *ab initio* calculations. *Chem. Phys. Lett.* **2020**, *752*, No. 137555.
(44) Hergert, W.; Geilhufe, R. M. *Group Theory in Solid State Physics and Photonics: Problem Solving with Mathematica*; Wiley-VCH: Weinheim, Germany, 2018.
(45) Geilhufe, R. M.; Hergert, W. GTPack: A Mathematica group theory package for application in solid-state physics and photonics. *Front. Phys.* **2018**, *6*, No. 86.
(46) Kendrick, B. K.; Hazra, J.; Balakrishnan, N. The geometric phase controls ultracold chemistry. *Nat. Commun.* **2015**, *6* (1), No. 7918.
(47) Huang, J.; Kendrick, B. K.; Zhang, D. H. Mechanistic insights into ultracold chemical reactions under the control of the geometric phase. *J. Phys. Chem. Lett.* **2021**, *12* (8), 2160−2165.
(48) Wang, J.; Xie, C.; Hu, X.; Guo, H.; Xie, D. Impact of geometric phase on dynamics of complex-forming reactions: H + O_2 → OH + O. *J. Phys. Chem. Lett.* **2024**, *15* (16), 4237−4243.
(49) Avdeenkov, A. V.; Bohn, J. L. Collisional dynamics of ultracold OH molecules in an electrostatic field. *Phys. Rev. A* **2002**, *66* (5), No. 052718.
(50) Stuhl, B. K.; Hummon, M. T.; Yeo, M.; Quéméner, G.; Bohn, J. L.; Ye, J. Evaporative cooling of the dipolar hydroxyl radical. *Nature* **2012**, *492* (7429), 396−400.
(51) Quéméner, G.; Bohn, J. L. Ultracold molecular collisions in combined electric and magnetic fields. *Phys. Rev. A* **2013**, *88* (1), No. 012706.
(52) Pastrana, M. R.; Quintales, L. A. M.; Brandao, J.; Varandas, A. J. C. Recalibration of a single-valued double many-body expansion potential energy surface for ground-state HO_2 and dynamics calculations for the O + OH → O_2 + H reaction. *J. Phys. Chem. A* **1990**, *94* (21), 8073−8080.
(53) Xu, C.; Xie, D.; Zhang, D. H.; Lin, S. Y.; Guo, H. A new *ab initio* potential-energy surface of HO_2(X^2A'') and quantum studies of HO_2 vibrational spectrum and rate constants for the H + O_2 ↔ O + OH reactions. *J. Chem. Phys.* **2005**, *122* (24), No. 244305.
(54) Varandas, A. J. C. Accurate combined-hyperbolic-inverse-power-representation of *ab initio* potential energy surface for the hydroperoxyl radical and dynamics study of O + OH reaction. *J. Chem. Phys.* **2013**, *138* (13), No. 134117.
(55) Wang, J.; An, F.; Chen, J.; Hu, X.; Guo, H.; Xie, D. Accurate full-dimensional global diabatic potential energy matrix for the two lowest-lying electronic states of the H + O_2 ↔ HO + O reaction. *J. Chem. Theory Comput.* **2023**, *19* (10), 2929−2938.
(56) Chen, W.; Xie, H.; Chen, Z.; Qu, Z.; Ren, H.; Li, X. Influence of singlet oxygen in H + O_2 collision reaction. *J. Phys. Chem. A* **2024**, *128* (34), 7226−7234.
(57) Harding, L. B. Theoretical studies of the hydrogen peroxide potential surface. 2. An *ab initio*, long-range, OH($^2\Pi$) + OH($^2\Pi$) potential. *J. Phys. Chem. A* **1991**, *95* (22), 8653−8660.
(58) Kuhn, B.; Rizzo, T. R.; Luckhaus, D.; Quack, M.; Suhm, M. A. A new six-dimensional analytical potential up to chemically significant energies for the electronic ground state of hydrogen peroxide. *J. Chem. Phys.* **1999**, *111* (6), 2565−2587.
(59) Karkach, S. P.; Osherov, V. I. *Ab initio* analysis of the transition states on the lowest triplet H_2O_2 potential surface. *J. Chem. Phys.* **1999**, *110* (24), 11918−11927.
(60) Braunstein, M.; Panfili, R.; Shroll, R.; Bernstein, L. Potential surfaces and dynamics of the O(^3P) + H_2O(X^1A_1) → OH($X^2\Pi$) + OH($X^2\Pi$) reaction. *J. Chem. Phys.* **2005**, *122* (18), No. 184307.
(61) Conforti, P. F.; Braunstein, M.; Braams, B. J.; Bowman, J. M. Global potential energy surfaces for O(^{3}P) + H_2O($^1A_1$) collisions. *J. Chem. Phys.* **2010**, *133* (16), No. 164312.
(62) Li, J.; Guo, H. A new *ab initio* based global HOOH($1^3A''$) potential energy surface for the O(^{3}P) + H_2O(X^1A_1) ↔ OH($X^2\Pi$) + OH($X^2\Pi$) reaction. *J. Chem. Phys.* **2013**, *138* (19), No. 194304.
(63) Li, J.; Dawes, R.; Guo, H. An accurate multi-channel multi-reference full-dimensional global potential energy surface for the lowest triplet state of H_2O_2. *Phys. Chem. Chem. Phys.* **2016**, *18* (43), 29825−29835.
(64) Coelho, D. V.; Brandão, J. A full dimensional potential for H_2O_2 (X^1A) covering all dissociation channels. *Phys. Chem. Chem. Phys.* **2017**, *19* (2), 1378−1388.
(65) Li, J.; Li, J. A full-dimensional potential energy surface and dynamics of the multichannel reaction between H and HO_2. *J. Phys. Chem. A* **2021**, *125* (7), 1540−1552.
(66) Casimir, H. B. G.; Polder, D. The influence of retardation on the London-van der Waals forces. *Phys. Rev.* **1948**, *73* (4), No. 360.
(67) McLachlan, A. D. Retarded dispersion forces between molecules. *Proc. R. Soc. London, Ser. A* **1963**, *271* (1344), 387−401.
(68) Werner, H.-J.; Knowles, P. J.; Knizia, G.; Manby, F. R.; Schuetz, M. Molpro: a general-purpose quantum chemistry program package. *WIREs Comput. Mol. Sci.* **2012**, *2* (2), 242−253.
(69) Werner, H.-J.; Knowles, P. J.; Manby, F. R.; Black, J. A.; Doll, K.; Heßelmann, A.; Kats, D.; Köhn, A.; Korona, T.; Kreplin, D. A.; et al. The Molpro quantum chemistry package. *J. Chem. Phys.* **2020**, *152* (14), No. 144107.
(70) Knowles, P. J.; Werner, H.-J. An efficient method for the evaluation of coupling coefficients in configuration interaction calculations. *Chem. Phys. Lett.* **1988**, *145* (6), 514−522.
(71) Werner, H. J.; Knowles, P. J. An efficient internally contracted multiconfiguration−reference configuration interaction method. *J. Chem. Phys.* **1988**, *89* (9), 5803−5814.
(72) Dunning, T. H. Gaussian basis sets for use in correlated molecular calculations. I. The atoms boron through neon and hydrogen. *J. Chem. Phys.* **1989**, *90* (2), 1007−1023, DOI: 10.1063/1.456153.
(73) Knowles, P. J.; Werner, H.-J. An efficient second-order MC SCF method for long configuration expansions. *Chem. Phys. Lett.* **1985**, *115* (3), 259−267.
(74) Werner, H. J.; Knowles, P. J. A second order multiconfiguration SCF procedure with optimum convergence. *J. Chem. Phys.* **1985**, *82* (11), 5053−5063.

https://doi.org/10.1021/jacsau.5c00966
JACS Au 2025, 5, 5079−5088

(75) Langhoff, P. W.; Karplus, M. Padé approximants for two- and three-body dipole dispersion interactions. *J. Chem. Phys.* **1970**, *53* (1), 233−250.
(76) Aidas, K.; Angeli, C.; Bak, K. L.; Bakken, V.; Bast, R.; Boman, L.; Christiansen, O.; Cimiraglia, R.; Coriani, S.; Dahle, P.; et al. The Dalton quantum chemistry program system. *WIREs Comput. Mol. Sci.* **2014**, *4* (3), 269−284.
(77) *Dalton, a molecular electronic structure program, Release Dalton2024.0-dev*. http://daltonprogram.org, 2024.
(78) Guan, Y.; Xie, C.; Yarkony, D. R.; Guo, H. High-fidelity first principles nonadiabaticity: diabatization, analytic representation of global diabatic potential energy matrices, and quantum dynamics. *Phys. Chem. Chem. Phys.* **2021**, *23* (44), 24962−24983.

https://doi.org/10.1021/jacsau.5c00966
JACS Au 2025, 5, 5079−5088